

# A strongly correlated electron model for the layered organic superconductors $\kappa$ -(BEDT-TTF)<sub>2</sub>X

Ross H. McKenzie\*

*School of Physics, University of New South Wales, Sydney 2052, Australia*

Published as *Comments Cond. Matt. Phys.* **18**, 309 (1998)

(Received March 17, 1998)

The fascinating electronic properties of the family of layered organic molecular crystals  $\kappa$ -(BEDT-TTF)<sub>2</sub>X where X is an anion (e.g., X=I<sub>3</sub>, Cu[N(CN)<sub>2</sub>]Br, Cu(SCN)<sub>2</sub>) are reviewed. These materials are particularly interesting because of similarities to the high- $T_c$  cuprate superconductors including unconventional metallic properties and competition between antiferromagnetism and superconductivity. The temperature dependence of electrical transport, optical, and nuclear magnetic resonance properties deviate significantly from those of a conventional metal. In particular, there appears to be an effective Fermi energy of the order of 100 K which is an order of magnitude smaller than predicted by band structure calculations. The results of quantum chemistry calculations suggest that a minimal theoretical model that can describe these materials is a Hubbard model on an anisotropic triangular lattice with one electron per site. Appropriate parameter values for the model imply that the electronic correlations are strong, significant magnetic frustration is present, and the system is close to a metal-insulator transition. Insight into the physics of this model can be obtained from recent studies of the Hubbard model using a dynamical mean-field approximation. They are consistent with a low effective Fermi energy and the unconventional temperature dependence of many of the properties of the metallic phase. Future directions are suggested for both theoretical and experimental studies.

The discovery of heavy fermion metals, high-temperature superconductivity in copper oxides, and colossal magnetoresistance in manganates has stimulated extensive experimental studies of these materials and extensive theoretical studies of strongly correlated electron models.<sup>1</sup> A key feature of the copper oxides (cuprates) is their layered or quasi-two-dimensional structure which enhances the effects of the interactions between the electrons and leads to metallic properties that are quite distinct from conventional metals.<sup>2,3</sup> Organic conductors based on the BEDT-TTF [bis-(ethylenedithia-tetrathiafulvalene)] molecule have been widely studied because prior to the discovery of fullerene superconductors they had the highest transition temperature ( $T_c \sim 10$  K) of an organic superconductor. The family  $\kappa$ -(BEDT-TTF)<sub>2</sub>X where X is an anion (X=Cu[N(CN)<sub>2</sub>]Br, for example) are particularly interesting because of similarities to the cuprates.<sup>4,5</sup> This article gives a brief review of these materials focussing on how the properties of the metallic phase are quite different from those of a conventional metal. The main purpose of this article is to argue that this is because these materials are strongly correlated electron systems<sup>6</sup> and that a model introduced by Kino and Fukuyama<sup>7</sup> may be the simplest possible theoretical model to describe them. Hopefully the article will stimulate more experimental and theoretical work on these exciting materials. Readers interested in a broader review of organic superconductors should consult recent monographs on the subject.<sup>8-10</sup>

## I. EXPERIMENTAL PROPERTIES

Organic molecular crystals with the formula (BEDT-TTF)<sub>2</sub>X consist of conducting layers of BEDT-TTF molecules sandwiched between insulating layers of anions X. The layered structure leads to highly anisotropic electronic properties. BEDT-TTF is a large planar molecule and the different possible packing patterns are denoted by different Greek letters<sup>11</sup>. The basic unit of the packing pattern in the  $\kappa$  phase is a “dimer” consisting of two BEDT-TTF molecules stacked on top of one another. Each dimer has one electron less than a full electronic shell because of charge transfer to the anions.

The family  $\kappa$ -(BEDT-TTF)<sub>2</sub>X has a particularly rich phase diagram as a function of pressure, temperature, and anion X=Cu[N(CN)<sub>2</sub>]Cl, Cu[N(CN)<sub>2</sub>]Br, and Cu(SCN)<sub>2</sub>, as shown in Fig. 1. A number of features of this diagram should be noted. (i) Antiferromagnetic and superconducting phases occur next to one another. (ii) At low pressures the metallic phase has properties that are quite distinct from conventional metals. (iii) The phase diagram is quite similar to that of the cuprates if pressure is replaced with doping. The properties of the different phases are now reviewed.

## A. Metal-insulator transition

In  $X=\text{Cu}[\text{N}(\text{CN})_2]\text{Cl}$  under moderate pressures (20-30 Mpa) as the temperature is lowered there is a first-order transition from an insulating into a metallic phase.<sup>12</sup> This transition also occurs at constant temperatures between 10 and 30 K as the pressure is increased. At ambient pressure  $X=\text{Cu}(\text{CN})_3$  is a paramagnetic insulator.<sup>13</sup> For pressures of 0.35 to 0.4 GPa there is a first order transition as the temperature is lowered. (For 0.35 GPa the resistivity decreases by five orders of magnitude at the transition). The temperature at which the metal insulator transition occurs increases with pressure. It will later be argued that this metal-insulator transition is a Mott-Hubbard transition driven by electron-electron interactions. However, it needs to be checked whether there is any structural change associated with this transition.  $\text{V}_2\text{O}_3$  undergoes a metal-insulator transition. Since there is a jump in one of the lattice constants at the transition its origin could be structural rather than electronic.

## B. Insulating antiferromagnetic phase

Evidence of antiferromagnetic ordering below 26 K is provided in  $X=\text{Cu}[\text{N}(\text{CN})_2]\text{Cl}$ <sup>14</sup> and deuterated  $X=\text{Cu}[\text{N}(\text{CN})_2]\text{Br}$ <sup>15</sup> by the observed splitting of proton nmr lines. The magnetic moment estimated from the magnitude of the splitting is  $(0.4 - 1.0)\mu_B$  per dimer. This large moment suggests that there are strong electron-electron interactions in these materials. Significant anisotropy is seen in the magnetic susceptibility below 26 K. Below 22 K there is weak ferromagnetic hysteresis with a saturation moment of about  $10^{-3}\mu_B$  per formula unit.<sup>16</sup> This small ferromagnetic moment could be due to a slight canting of the antiferromagnetic moments.<sup>17</sup> Antiferromagnetic resonance<sup>18</sup> results are consistent with an easy plane antiferromagnet with Dzyaloshinskii-Moriya interaction. The antiferromagnetic phase becomes unstable under moderate pressures of about 300 bar. It can be stabilised and enhanced by a magnetic field perpendicular to the layers of the order of a few tesla.<sup>19</sup>

The observed phase diagram at the boundary of the superconducting and insulating phases is actually more complex than shown in Fig. 1. For example, coexistence of superconductivity and antiferromagnetic phases has been observed.<sup>20,12,15</sup> As the temperature is lowered a superconductor to insulator transition is observed.

## C. Metallic phase

Many of the properties of the metallic phase have a temperature dependence that is quite distinct from that of conventional metals. Yet at low temperatures (less than about 30 K) some properties are similar to those of a conventional metal, but with a Fermi energy of the order of 100 K. This is almost an order of magnitude smaller than predicted by band structure calculations. Application of pressures of the order of 10 kbar restores conventional metallic properties over the full temperature range. The details of different properties are now reviewed.

*Optical conductivity.* Infrared<sup>21,22</sup> and microwave<sup>23</sup> measurements of the frequency dependent conductivity  $\sigma(\omega)$  of  $X=\text{Cu}(\text{SCN})_2$ ,  $X=\text{Cu}[\text{N}(\text{CN})_2]\text{Br}$ , and  $X=\text{I}_3$ <sup>24</sup> deviate from the Drude behavior found in conventional metals. At room temperature  $\sigma(\omega)$  is dominated by a broad peak around 300 or 400 meV (depending on the polarization and anion X) with a width of about 150 meV. Even down to 50 K no “Drude-like” peak at zero frequency is present (see Fig. 2). At 25 K the high energy peak decreases slightly in temperature and a “Drude-like” peak but can only be fit to a Drude form if the scattering rate and effective mass are frequency dependent.<sup>21</sup>

*Nuclear magnetic resonance.* In a conventional metal, the Knight shift  $K$  is proportional to the density of states at the Fermi energy and is independent of temperature.<sup>25</sup> In contrast, in  $X=\text{Cu}[\text{N}(\text{CN})_2]\text{Br}$  the Knight shift decreases significantly below about 50 K, suggesting a suppression of the density of states or “pseudogap” near the Fermi energy.<sup>26,27</sup> In conventional metals the NMR relaxation rate  $1/T_1$  obeys Korringa’s law:<sup>25</sup>  $1/(T_1TK^2)$  is independent of temperature and a universal number. The relaxation rate is five to ten times larger than expected from Korringa’s law and is strongly temperature dependent:  $1/(T_1T)$  has a peak in the range 10 to 50 K, depending on how close the system is to the metal-insulator transition.<sup>26,28,29</sup> Above 50 K the relaxation rate is similar for  $X=\text{Cu}[\text{N}(\text{CN})_2]\text{Cl}$ ,  $\text{Cu}[\text{N}(\text{CN})_2]\text{Br}$  and  $X=\text{Cu}(\text{NCS})_2$ <sup>28,29</sup>. The above behavior has some similarities to the temperature dependence of the nmr properties of the underdoped cuprates.<sup>30</sup> As the pressure is increased to four kilobars the NMR properties become more like those of a conventional metal: the Knight shift and  $1/(T_1T)$  become independent of temperature.<sup>27</sup>

*Temperature dependence of the resistance.* Unlike a conventional metal the resistance does not monotonically increase with temperature. It is a maximum at  $T_{max}$  where  $T_{max} \simeq 100$  K for  $X=\text{Cu}(\text{NCS})_2$ . With increasing pressure  $T_{max}$  increases and the peak disappears at high pressures.<sup>15</sup> From about 30 K down to the superconducting transition temperature the resistance decreases quadratically with temperature<sup>31</sup>

$$\rho(T) = \rho_0 + AT^2 \quad (1)$$

Such a temperature dependence is characteristic of metals in which the dominant scattering mechanism is the interactions of the electrons with one another and is observed in transition metals and heavy fermions. In those systems the Kadowaki-Woods rule<sup>32,33</sup> relates the coefficient  $A$  in (1) to the linear coefficient for the specific heat,  $\gamma$ :  $A/\gamma^2 = \text{constant}$ . The constant is  $4.0 \times 10^{-13} \Omega \text{cm} (\text{mol/mJ})^2$  for transition metals, and  $1.0 \times 10^{-11} \Omega \text{cm} (\text{mol/mJ})^2$  for heavy fermions and for transition metal oxides near the Mott-Hubbard transition<sup>34</sup>. In the organics the ratio is 5 to 200 times larger than predicted by this law<sup>35,31</sup>. It has been suggested that this discrepancy implies that the dominant scattering mechanism is phonons.<sup>35,36</sup> In some strong coupling superconductors<sup>37</sup> and dirty metallic films<sup>38</sup> a  $T^2$  resistivity is observed. If interference between electron-phonon scattering and disorder is taken into account theory predicts that  $A \simeq \alpha \rho(0)/\theta_D^2$  where  $\alpha \sim 0.01 - 0.1$ , and  $\rho(0)$  is the residual resistivity due to disorder. Comparing to the data on  $\text{X}=\text{Cu}(\text{SCN})_2$  in Ref. 31, the value of  $A$  predicted by this expression is several orders of magnitude smaller than observed.

*Mean-free path and Mott's minimum conductivity.*<sup>39</sup> If the electronic mean-free path is less than a lattice constant than the idea of electronic transport by electrons with well-defined wavevector is no longer meaningful.<sup>40</sup> Then the material should act as an insulator with a resistance that drops with increasing temperature; to the contrary it remains a metal with an increasing resistance. If the mean-free path is of the order of a lattice constant then for a quasi-two dimensional Fermi surface the intralayer conductivity will be approximately,

$$\sigma_{min} \sim \frac{e^2}{h} \frac{B}{c} \quad (2)$$

where  $c$  is the interlayer spacing and  $B$  is a constant of order one. For  $c \sim 10 \text{\AA}$  this gives  $\sigma_{min} \sim 10^3 (\Omega \text{cm})^{-1}$ . The intralayer conductivity of  $\text{X}=\text{Cu}(\text{NCS})_2$  is comparable to this at 30 K and is three orders of magnitude smaller at 100 K.<sup>31</sup> However, from 30 to 100 K, the resistance increases with temperature, characteristic of a metal. Hence, these materials can be classified as “bad metals.”<sup>41</sup>

*Hall resistance.* In a conventional metal the Hall resistance is a measure of the number of charge carriers and is independent of temperature above about  $0.3\theta_D$ , where  $\theta_D$  is the Debye temperature.<sup>42</sup> (Specific heat measurements<sup>43</sup> suggest  $\theta_D \sim 200$  K in the  $\kappa$  salts). The Hall resistance of  $\text{X}=\text{Cu}(\text{SCN})_2$  is weakly temperature dependent above 80 K but increases by a factor of three as the temperature is decreased from 80 K down to the superconducting transition temperature (10 K).<sup>44</sup> Hall measurements on  $\text{X}=\text{Cu}[\text{N}(\text{CN})_2]\text{Br}$  and  $\text{X}=\text{Cu}[\text{N}(\text{CN})_2]\text{Cl}$  at ambient pressure<sup>45</sup> also found a strong temperature dependence but were complicated by long-term sample resistance relaxation. Recent measurements on the  $\text{X}=\text{Cu}[\text{N}(\text{CN})_2]\text{Cl}$  salt under pressure also found a strong temperature dependence<sup>20</sup>. However, the ratio of the longitudinal resistance  $R_{xx}$  to the Hall resistance  $R_H$  has a simple quadratic temperature dependence up to 100 K:

$$\cot \theta_H \equiv \frac{R_{xx}}{R_H} = \alpha T^2 + C. \quad (3)$$

$\theta_H$  is known as the Hall angle. Similar behavior is found in the cuprate superconductors<sup>46</sup>. It has been suggested that in the cuprates that there are two distinct scattering times and that these have a different temperature dependence.<sup>47,48</sup> The Hall resistance involves the product of the two scattering rates. This hypothesis needs to be tested in the organics by checking if  $R_{xx}^2/R_H$  is independent of temperature.

*Thermoelectric power.* In a conventional metal the thermoelectric power is given by

$$S = \frac{\pi^2}{3e} \frac{k_B^2 T}{E_F}. \quad (4)$$

where  $k_B$  is Boltzmann's constant,  $e$  is the electronic charge, and  $E_F$  is the Fermi energy. The Fermi energy estimated from comparing this expression to measurements<sup>49</sup> on  $\text{X}=\text{Cu}[\text{N}(\text{CN})_2]\text{Br}$  is several times smaller than predicted by Hückel band structure calculations. Furthermore, the thermopower is not linear in temperature above 30 K and has a peak around 100 K (as does the resistivity) and is similar in magnitude and temperature dependence to the cuprates<sup>50</sup>.

*Specific heat.* The low-temperature specific heat of  $\text{X}=\text{Cu}[\text{N}(\text{CN})_2]\text{Br}$  and  $\text{X}=\text{Cu}(\text{SCN})_2$  have been measured<sup>51,43</sup> at ambient pressure and under a magnetic field of 10 tesla (to destroy the superconductivity). The specific heat coefficients  $\gamma$  are  $22 \pm 3 \text{ mJ K}^{-2} \text{ mol}^{-1}$  and  $25 \pm 3 \text{ mJ K}^{-2} \text{ mol}^{-1}$ , respectively, about 2.5 times larger than predicted by Hückel band structure calculations.<sup>52</sup>

*Magnetic susceptibility.* In a conventional metal this is independent of energy for temperatures much less than the Fermi energy. For the  $\kappa$  salts the susceptibility  $\chi$  is almost independent of temperature above 50 K but decreases slightly below 50 K.<sup>52</sup>

*Wilson ratio.* The dimensionless quantity  $R \equiv 4\pi^2 k_B^2 \chi(0) / (3(g\mu_B)^2 \gamma)$  where  $g \simeq 2$  is the gyro-magnetic ratio and  $\mu_B$  is the Bohr magneton. For a non-interacting Fermi gas  $R = 1$  and for the Kondo model  $R = 2$ . For heavy fermion metals it is in the range one to three.<sup>53</sup> For both  $X=\text{Cu}[\text{N}(\text{CN})_2]\text{Br}$  and  $X=\text{Cu}(\text{SCN})_2$  it is  $1.5 \pm 0.2$ .

*Magneto-oscillations.* The temperature dependence of the amplitude of Shubnikov - de Haas and de Haas - van Alphen oscillations can be used to deduce the effective mass,  $m^*$ , of the charge carriers associated with various orbits on the Fermi surface.<sup>9</sup> Values obtained for the  $\beta$  orbit include  $m^*/m_e = 5.4 \pm 0.1, 7.1 \pm 0.5, 3.9 \pm 0.1$  for  $X=\text{Cu}[\text{N}(\text{CN})_2]\text{Br}$ ,<sup>54</sup>  $X=\text{Cu}(\text{SCN})_2$ ,<sup>55</sup> and  $X=\text{I}_3$ ,<sup>59</sup> respectively. For the  $\alpha$  orbit in  $X=\text{Cu}(\text{SCN})_2$  a value of  $3.3 \pm 0.1$  has been obtained.<sup>55-58</sup> Under a pressure of 20 kbar this effective mass decreases to  $1.5m_e$ .<sup>56</sup> The rapid decrease in the effective mass with increasing pressure was correlated with the decrease in the superconducting transition temperature. A cyclotron resonance measurement (which should measure the bare mass and not the effective mass<sup>60</sup>) on  $X=\text{Cu}(\text{SCN})_2$  gives a mass of  $1.2m_e$ .<sup>61</sup>

The measured effective masses are two to four times larger than predicted by Hückel band-structure calculations that ignore the interactions between the electrons. Calculations using the local-density approximation (LDA) for  $X=\text{Cu}[\text{N}(\text{CN})_2]\text{Br}$  give a band width a factor of two smaller than Hückel.<sup>62</sup>

The fact that the effective mass, specific heat, and magnetic susceptibility are significantly larger than predicted by band structure calculations suggest that the band width is narrowed by many-body effects.

## D. Superconducting phase

There is increasing evidence that, like in the cuprates,<sup>63</sup> the pairing of electrons in the superconducting state involves a different symmetry state than in conventional metals. Below I briefly review the evidence, pointing out where controversy exists.

*Nuclear magnetic resonance.* The NMR relaxation rate  $1/T_1$  does not have a Hebel-Slichter peak below  $T_c$ . At low temperatures,  $1/T_1 \sim T^3$ ,<sup>26,64</sup> instead of the exponentially activated behavior found in conventional superconductors. This power law behavior suggests there are nodes in the gap.

*Specific heat.* At low temperatures the electronic specific heat of  $X=\text{Cu}[\text{N}(\text{CN})_2]\text{Br}$  has a power law dependence on temperature, in contrast to the exponentially activated dependence of conventional superconductors. In a magnetic field  $B$  perpendicular to the layers the electronic specific heat is linear in temperature with coefficient  $\gamma \sim B^{1/2}$ .<sup>65</sup> This is the behavior predicted for a clean two-dimensional superconductor with nodes in the gap.<sup>66</sup> In contrast, in a conventional superconductor  $\gamma \sim B$ .

*Magnetic penetration depth.* There is controversy about its temperature dependence. dc magnetisation measurements on  $X=\text{Cu}(\text{SCN})_2$  have been fitted to the exponentially activated temperature dependence expected for an s-wave superconductor.<sup>67</sup> In contrast, muon spin rotation ( $\mu\text{SR}$ ) measurements on  $X=\text{Cu}(\text{SCN})_2$  and  $X=\text{Cu}[\text{N}(\text{CN})_2]\text{Br}$  show a linear temperature dependence with temperature.<sup>68</sup> Other  $\mu\text{SR}$  measurements are consistent with an s-wave order parameter.<sup>69</sup> Surface impedance measurements on  $X=\text{Cu}(\text{SCN})_2$  and  $X=\text{Cu}[\text{N}(\text{CN})_2]\text{Br}$  give a penetration depth whose temperature dependence is consistent with s-wave pairing.<sup>23</sup> Furthermore, the real part of the conductivity versus temperature has a ‘coherence’ peak just below  $T_c$ , as in conventional superconductors.

*Upper critical field  $H_{c2}$ .* The  $H_{c2}$  versus temperature curve for  $X=\text{Cu}(\text{SCN})_2$  shows upper curvature near  $T_c$ . The large slope near  $T_c$  suggests that at low temperatures  $H_{c2}$  could exceed the Pauli limit (the field at which BCS theory predicts singlet Cooper pairs should be broken).<sup>70,71</sup>

*Vortex dynamics.* Vibrating reed studies of  $X=\text{Cu}[\text{N}(\text{CN})_2]\text{Br}$  in magnetic fields less than one tesla suggest anomalous vortex dynamics and the possibility of unconventional superconductivity.<sup>72</sup>

## II. THEORY

I now argue that a theoretical model introduced by Kino and Fukuyama<sup>7</sup> captures enough of the essential physics of these materials to describe them, at least at the semi-quantitative level. Insight into the model is obtained by considering its various limits and what is known about similar models.

### A. Band structure

The arrangement of the BEDT-TTF molecules in the  $\kappa$  crystal structure and the dominant intermolecular hopping integrals are shown in Figure 3. Table I shows values for these integrals found from various quantum chemistry calculations for different anions. The intradimer hopping  $t_{b_1}$  is more than two times larger than the interdimer

integrals,  $t_p$  and  $t_q$  along the  $c + a$  direction, and  $t_{b_2}$  along the  $c$  direction. The dimer bonding and antibonding orbitals are split by approximately  $2t_{b_1}$  and so the mixing between bonding and antibonding orbitals can be neglected and the interdimer hoppings can be treated as a perturbation. Focusing on antibonding orbitals, each dimeric site has two nearest neighbors along the  $c$  direction (interaction  $t_1 \equiv t_{b_2}/2$ ), and four next-nearest neighbors along the  $c \pm a$  directions (interaction  $t_2 \equiv (t_p + t_q)/2$ ). The dimer model is shown in Fig. 4 (compare Figures 1 and 6 in Ref. 24 and Figure 13 in Ref. 7) Note that each lattice site has hopping to six neighbours and so the lattice has the same co-ordination as the triangular lattice. Since each dimer has three electrons (or one hole), the upper (conduction) band is half-filled.

If the interactions between electrons are neglected (which it will be argued below is not justified) then the model is just a tight-binding model and the dispersion relation for the half-filled band is

$$E(k_a, k_c) = 2t_1 \cos(k_c c) + 4t_2 \cos\left(\frac{k_a a}{2}\right) \cos\left(\frac{k_c c}{2}\right) \quad (5)$$

This band structure reproduces the main features of bands calculated using the extended Hückel approximation<sup>73,74</sup>. Bands calculated using the local-density approximation (LDA) for  $X=\text{Cu}(\text{NCS})_2$  and  $X=\text{Cu}[\text{N}(\text{CN})_2]\text{Br}$  are also similar apart from an overall bandwidth narrowing.<sup>62</sup> The band structure (5) has been used to model the results of Shubnikov - de Haas oscillations measurements<sup>56</sup> on  $X=\text{Cu}(\text{NCS})_2$  and reflectance measurements<sup>24</sup> on  $X=\text{I}_3$ .

### B. Estimates of the Coulomb repulsion

To test whether these materials can be described by a tight-binding model which neglects electron-electron interactions the effective Coulomb repulsion between two electrons in the anti-bonding orbital on a BEDT-TTF dimer is now estimated. Quantum chemistry calculations<sup>75-77</sup> estimate that the Coulomb repulsion between two electrons on a *single* BEDT-TTF molecule  $U_0$  is about 4-5 eV. These calculations neglect the screening effects present in the solid state and so the actual  $U_0$  may actually be smaller.  $U_0$  has been estimated from optical experiments to be 0.7 eV in (BEDT-TTF)HgBr<sub>3</sub><sup>78</sup> and in  $\alpha'$ -(BEDT-TTF)<sub>2</sub>Ag(CN)<sub>2</sub> to be 1.3 eV.<sup>79</sup>

If  $E_0(N)$  denotes the ground state energy of  $N$  electrons on a dimer then<sup>80,7</sup>  $E_0(2) = \frac{1}{2}(U_0 - (U_0^2 + 16t_{b_1}^2)^{1/2})$ ,  $E_0(3) = U_0 - t$ , and  $E_0(4) = 2U_0$ . The effective Coulomb repulsion  $U$  between two electrons on a dimer is then

$$U = E_0(4) + E_0(2) - 2E_0(3) = 2t_{b_1} + \frac{1}{2}(U_0 - (U_0^2 + 16t_{b_1}^2)^{1/2}) \quad (6)$$

If  $U_0 \gg 4t_{b_1}$  the effective repulsion between two holes on a dimer is approximately  $2t_{b_1}$  (See Figure 5). However, if  $U_0 \sim 4t_{b_1} \sim 1$  eV then  $U \sim 0.3$  eV. The optical conductivity data shown in Fig. 2 is consistent with this estimate. This value of  $U$  is comparable to the band width of the tight binding model and so suggests that correlation effects are important.

### C. A minimal model: the dimer Hubbard model

Based on the above discussion we suggest that a minimal theoretical model to describe the  $\kappa$ -(BEDT-TTF)<sub>2</sub>X crystals is the following Hamiltonian,<sup>7</sup>

$$H = -t_1 \sum_{\langle \mathbf{ij} \rangle, \sigma} (c_{\mathbf{i}, \sigma}^\dagger c_{\mathbf{j}, \sigma} + h.c.) - t_2 \sum_{\langle \mathbf{in} \rangle, \sigma} (c_{\mathbf{i}, \sigma}^\dagger c_{\mathbf{n}, \sigma} + h.c.) + U \sum_{\mathbf{i}} (n_{\mathbf{i}\uparrow} - \frac{1}{2})(n_{\mathbf{i}\downarrow} - \frac{1}{2}) + \mu \sum_{\mathbf{i}, \sigma} n_{\mathbf{i}\sigma}, \quad (7)$$

where  $c_{\mathbf{i}, \sigma}^\dagger$  creates a hole at dimer site  $\mathbf{i}$  with spin projection  $\sigma$ ,  $n_{\mathbf{i}\sigma}$  is the hole number operator. The sum  $\langle \mathbf{ij} \rangle$  runs over pairs of nearest neighbor lattice sites in the horizontal direction, and the sum  $\langle \mathbf{in} \rangle$  runs over pairs of lattice sites along the diagonals.  $U$  is the on-site Coulombic repulsion on a single dimer (estimated in the previous section), and  $\mu$  is the chemical potential. At half-filling  $\mu$  may be non-zero due to the absence of particle-hole symmetry if both  $t_1$  and  $t_2$  are non-zero.

If there are strong correlations on each dimer then the amplitude for hopping between neighbouring dimers,  $t_1$  and  $t_2$ , are not simply given by  $t_1 = t_{b_2}/2$  and  $t_2 = (t_p + t_q)/2$ . The correct amplitude involves the overlap of a one hole state with the anti-bonding orbital creation operator acting on a two-hole state.<sup>81</sup> A straight-forward calculation gives

$$\frac{t_1}{t_{b_2}} = \frac{t_2}{(t_p + t_q)} = \frac{1}{2\sqrt{2}} (\cos \theta - \sin \theta) \quad (8)$$

where

$$\tan \theta = \frac{U_0}{4t_{b1}} - \left( \left( \frac{U_0}{4t_{b1}} \right)^2 + 1 \right)^{1/2} \quad (9)$$

If  $U_0 \gg 4t_{b1}$  then correlations on the dimer reduce the inter-dimer hopping by a factor of  $1/\sqrt{2}$ .

Various limits of the model (7) are now considered leading to the speculative phase diagram shown in Fig. 6.

An important property of this model is that at half-filling a non-zero  $U$  is required for an insulating phase. A finite  $U$  is required because if  $t_1$  and  $t_2$  are both non-zero the nesting of the Fermi surface is not perfect. In the Hartree-Fock approximation Kino and Fukuyama<sup>7</sup> found that for  $2t_1 = t_2$ , the critical value is  $U_c/t_2 \simeq 3$ .

If  $t_1 = t_2 = t$  the model becomes the Hubbard model on a triangular lattice, after a rescaling of the lattice constants. Although there have been a number of studies of this model at half filling, no clear consensus of the phase diagram has been reached except that the ground state should be a paramagnetic metal for small  $U/t$  and an insulator for large  $U/t$ . The model has been studied by techniques including the Hartree-Fock approximation (which predicts  $U_c/t \simeq 5$ ),<sup>82</sup> the slave boson technique,<sup>83</sup> and exact diagonalization of small clusters.<sup>84</sup> The slave boson technique predicts that between the paramagnetic metal and insulating antiferromagnetic phase that there is semimetallic linear commensurate spin-density-wave phase for  $6.9 < U/t < 7.8$ .<sup>85</sup> In order to allow for the slightly different band structure associated with the lattice considered here these critical values of  $U$  must be divided by  $\sqrt{3}$ . Both the Hartree-Fock and slave-boson (mean-field) approximations tend to underestimate the effect of fluctuations and so the actual critical  $U$  may be larger than the above values.

The estimate of  $U$  in the previous section and the parameter values given in Table I for various  $\kappa$ -(BEDT-TTF)<sub>2</sub>X crystals suggest that  $U/(t_1 + t_2) \sim 3 - 6$  and so these materials may be close to the metal-insulator transition.

#### D. Strong coupling limit for the insulating phase

If  $U \gg t_1, t_2$  then the ground state is an insulator and a standard strong-coupling expansion<sup>86</sup> for the Hamiltonian (7) implies that the spin degrees of freedom are described by the spin- $\frac{1}{2}$  Heisenberg model

$$H = J_1 \sum_{\langle \mathbf{ij} \rangle} \mathbf{S}_i \cdot \mathbf{S}_j + J_2 \sum_{\langle \mathbf{in} \rangle} \mathbf{S}_i \cdot \mathbf{S}_n \quad (10)$$

where  $\mathbf{S}_i$  denotes a spin operator on site  $\mathbf{i}$ ,  $J_1 = t_1^2/U$  and  $J_2 = t_2^2/U$ . Again, the sum  $\langle \mathbf{ij} \rangle$  runs over pairs of nearest neighbor lattice sites in the horizontal direction, and the sum  $\langle \mathbf{in} \rangle$  runs over pairs of lattice sites along the diagonals.  $J_1$  and  $J_2$  are competing interactions leading to magnetic frustration. The parameter values in Table I suggest that  $J_1/J_2 \sim 0.3 - 1$  and so magnetic frustration will play an important role in these materials. This model has some similarities to a model considered for the layered titanate  $\text{Na}_2\text{Ti}_2\text{Sb}_2\text{O}$  and with possible spin liquid ground states.<sup>87</sup>

Insight can be gained by considering various limits of this model. If  $J_1 = 0$  then the model reduces to the Heisenberg model on a square lattice. At zero temperature there will be long range Neel order with a magnetic moment of  $0.6\mu_B$ .<sup>86</sup> If  $J_1$  is non-zero but small it will introduce a small amount of magnetic frustration which will reduce the magnitude of the magnetic moment in the Neel state. The spin structure is shown in Fig. 7 the same as that proposed for the antiferromagnetic phase of deuterated  $\text{X}=\text{Cu}[\text{N}(\text{CN})_2]\text{Br}$  based on nmr<sup>15</sup>. As the ratio  $J_1/J_2$  varies the wave vector associated with the antiferromagnetic order may also vary. There is the possibility of commensurate-incommensurate transitions.

If  $J_1 = J_2$  then the model reduces to the Heisenberg model on a triangular lattice. There has been some controversy about the ground state of this model. Anderson<sup>88</sup> originally suggested that the ground state was a “spin liquid” with no long-range magnetic order. However, recent numerical work suggests that there is long-range order but the quantum fluctuations are so large due to the magnetic frustration that the magnetic moment may be an order of magnitude smaller than the classical value.<sup>89</sup>

If  $J_2 = 0$  then the model reduces to a set of decoupled Heisenberg antiferromagnetic chains which do not have long-range order.<sup>86</sup> If  $J_2$  is non-zero but small the chains are weakly coupled. The case of only two chains corresponds to the “zig-zag” spin chain which is equivalent to a single chain with nearest-neighbour and next-nearest neighbour exchange,  $J_2$  and  $J_1$ , respectively. (Unfortunately, the definition of  $J_1$  and  $J_2$  is the opposite of that normally used). This spin chain has been extensively studied and is well understood.<sup>90</sup> In the limit of interest here,  $J_2 \ll J_1$ , there is a gap in the spectrum  $\Delta \sim \exp(-\text{const.} J_1/J_2)$  and there is long-range dimer order. We speculate that this “spin gap” is still present in the many chain limit.

Based on the above discussion a schematic phase diagram for the model (7) at half filling and at zero temperature has been drawn in Fig. 6. The possibility of superconductivity near the metal-insulator transition is suggested only on the basis of comparison with the experimental phase diagram.

### E. The effect of pressure

A very important challenge is to understand how varying the pressure changes the ground state of the system. The experimental phase diagram shown in Fig. 1 certainly suggests that pressure reduces the electronic correlations. In most strongly correlated systems pressure increases the band width by more than the Coulomb repulsion and so reduces the effect of correlations. The effect of pressure in this system is more subtle because the Coulomb repulsion  $U$  is related to the hopping integral  $t_{b_1}$  (see equation (6)) which will increase with pressure and the ratio  $t_1/t_2$  may vary with pressure and could drive the metal-insulator transition. Rahal et al.<sup>91</sup> measured the crystal structure of  $X=\text{Cu}(\text{NCS})_2$  at room temperature and pressures of 1 bar and 7.5 kbar. They then performed Hückel calculations of the hopping integrals for the corresponding crystal structures. The results, given in Table I, suggest that the amount of magnetic frustration decreases as the pressure increases. In contrast to the work of Rahal et al. a more heuristic approach was taken in an earlier study by Campos et al.<sup>92</sup> In order to fit experimental data for the pressure dependence of the Fermi surface area deduced from magneto-oscillation frequencies, they made assumptions about how the BEDT-TTF molecules move relative to one another as the pressure varies. They found an increase in  $t_1/t_2$  with pressure.

Assuming that the Coulomb repulsion on a single BEDT-TTF molecule  $U_0$  does not vary significantly with pressure then equation (6) implies

$$\frac{dU}{dP} = 2 \frac{dt_{b_1}}{dP} \left( 1 - \frac{4t_{b_1}}{(U_0^2 + 16t_{b_1}^2)^{1/2}} \right) \quad (11)$$

If  $U_0 \gg 4t_{b_1}$  then  $U$  will increase with pressure at about the same rate as  $t_{b_1}$  which is similar to the rate at which  $t_1$  and  $t_2$  increase. This could mean that the correlations change little with pressure. However, if  $U_0 \sim 4t_{b_1}$  then the second term in (11) reduces the rate at which  $U$  increases and so correlation effects can decrease with pressure. The uncertainty in the variation of the parameters with pressure is sufficiently great that more work is required before definitive answers can be obtained about this important question of how the ground state changes with pressure.

### F. Dynamical mean-field theory for the Hubbard model

Some insight into the physics of the organics, particularly the existence of a low-energy scale in the metallic phase, can be gained by briefly reviewing progress that has been made in the past few years in understanding the Mott-Hubbard metal-insulator transition.<sup>93</sup> This has been done by studying the Hubbard model in a dynamical mean-field approximation which becomes exact in the limit of either large *lattice connectivity* or *spatial dimensionality*. This approximation maps the problem onto a single impurity problem that must be solved self-consistently. While time-dependent fluctuations are captured by this approximation spatially-dependent fluctuations are not captured. Some important physics that emerges from these studies is that there is an important low-energy scale  $T_0$  which is much smaller than the half-bandwidth  $D$  and the Coulomb repulsion  $U$ . This energy scale is the analogue of the Kondo temperature for the impurity problem. If there is significant magnetic frustration the Neel temperature for antiferromagnetic ordering is suppressed. Then at half filling and at fixed temperature  $T < T^* \simeq 0.05D$  as  $U$  is increased there is a first-order phase transition from a paramagnetic metallic phase to a paramagnetic insulating phase at  $U = U_c \sim 3D$ .

In the metallic phase the density of states  $\rho(\omega)$  contains peaks at energies  $\omega = -U/2$  and  $+U/2$  which correspond to the lower and upper Hubbard bands, respectively and involve incoherent states. These peaks are broad and have width of order  $D$ . At temperatures less than  $T_0$  a new quasi-particle peak with width of order  $T_0$  forms at  $\omega = 0$  (Figure 39 in Reference 93). The spectral weight of the peak vanishes as the metal-insulator transition is approached. The quasi-particle band involves coherent states that form a Fermi liquid. This means that the self energy  $\Sigma(\omega)$  is independent of momentum has the energy dependence,  $\text{Re}\Sigma(\omega) = U/2 + (1 - 1/Z)\omega + O(\omega^3)$  and  $\text{Im}\Sigma(\omega) = -B\omega^2 + O(\omega^4)$ .  $Z$  is the quasiparticle residue and is related to the effective mass  $m^*$  by  $m^*/m_e = 1/Z$ . As the metal-insulator transition is approached  $T_0 \rightarrow 0$  and  $Z \rightarrow 0$ .<sup>94</sup> The consequences of the above picture for the temperature dependence of different physical quantities for metals in close proximity to the metal-insulator transition are now briefly described.

*Optical conductivity.*<sup>95,97</sup> For temperatures  $T$  larger than  $T_0$  the optical conductivity is small near zero-frequency and has a broad peak at  $\omega = U$ , corresponding to transitions between the lower and upper Hubbard bands. For  $T < T_0$  a Drude-like peak forms at zero-frequency and there is a new-shoulder at  $\omega \sim U/2$ . The latter peak corresponds to transitions from the quasi-particle band to the upper Hubbard band and from the lower Hubbard band to the quasi-particle band. The total spectral weight increases as the temperature decreases. This picture has been used to explain the temperature dependence of the optical conductivity of vanadium oxides.<sup>95,98,99</sup> If this picture is used to explain the data shown in Fig. 2 then the Coulomb repulsion  $U$  is estimated to be about 250 to 350 meV. This is roughly consistent with the estimates in Section II B.

*Resistivity.* The temperature dependence of the dc resistivity  $\rho(T)$  is not monotonic. It has a peak at a temperature of the order of  $T_0$ , and decreases rapidly below the peak. (See Figure 9 in Reference 97, Figure 2 in Reference 100, and the inset of Figure 2 in Reference 95).

*Mean-free path.* Since coherent quasiparticles only exist for  $T < T_0$  it is not required that the mean-free path be larger than a lattice constant at high temperatures. Thus, it is possible for the resistivity to increase with temperature and be larger than the Mott minimum resistivity.

*Fermi liquid regime.* The properties of the low temperature range ( $T < T_0$ ) in which the metal has Fermi liquid properties is now considered.

*Specific heat.* In the Fermi liquid regime the linear coefficient is<sup>94</sup>

$$\gamma = \frac{2\pi k_B^2}{3ZD} \quad (12)$$

where  $Z = 0.9(1 - U/U_c)$  is the quasi-particle weight. The effective Fermi energy is  $\epsilon_F^* = ZD$ .

*Effective mass.* This is related to the quasiparticle weight  $Z$  by

$$\frac{m^*}{m_e} = \frac{1}{Z} \quad (13)$$

and diverges at the transition, consistent with the Brinkman-Rice scenario<sup>96</sup> for the metal-insulator transition.

*Resistivity.* At low temperatures  $\rho(T) \sim AT^2$ , characteristic of a Fermi liquid. Near the Mott-Hubbard transition the coefficient  $A$  is related to the specific heat coefficient  $\gamma$  by  $A/\gamma^2 = (2.3a) \times 10^{-12}$  ohm cm (mol/mJ)<sup>2</sup> where  $a$  is the lattice constant in Å of a three-dimensional system.<sup>94</sup>

*Magnetic susceptibilities.* The uniform susceptibility (in units in which  $g\mu_B = 2$ ) is

$$\chi(q=0) = \frac{1}{0.45\epsilon_F^* + J} \quad (14)$$

where  $J \equiv D^2/2U$  is the magnetic exchange energy. Note that this does *not* diverge at the transition. In contrast, the local susceptibility

$$\chi_{loc} \equiv \sum_q \chi(q) = \frac{4.7}{\epsilon_F^*} \quad (15)$$

The local susceptibility can be related to the spin-echo decay rate  $1/T_{2G}$ .<sup>103</sup>

*The Wilson ratio.* This is only universal for the local susceptibility.

$$R \equiv \frac{\chi_{loc}/\chi_{loc}^{free}}{\gamma/\gamma^{free}} = 2.8 \quad (16)$$

where  $\chi_{loc}^{free}$  and  $\gamma^{free}$  are the values in the absence of interactions.

*The nmr relaxation rate.* The spin relaxation rate  $1/T_1$  depends linearly on temperature

$$\frac{1}{T_1 T} = \lim_{\omega \rightarrow 0} \frac{\chi_{loc}''(\omega)}{\omega} = \frac{12.5}{(\epsilon_F^*)^2} \quad (17)$$

This could be combined with (15) to give a generalised Korringa-type relation. However, this is not directly relevant to nmr since the Knight shift  $K$  is proportional to the uniform susceptibility, not the local susceptibility. The Korringa ratio  $1/(T_1 T K^2)$  will diverge at the transition.

I am unaware of calculations of the complete temperature dependence of  $1/(T_1 T)$ , the thermopower, and Hall resistance. However, these quantities have been calculated for a doped Mott insulator. It was found<sup>101</sup> that  $1/T_1$

versus temperature had a maximum at a temperature of the order of  $T_0$ . The thermopower versus temperature curve<sup>101</sup> has a maximum at a temperature of the order of  $T_0$  at which its magnitude is of order  $40 \mu\text{V/K}$ . The Hall resistance is temperature dependent.<sup>101,102</sup> The Hall angle has an approximately quadratic temperature dependence.<sup>101</sup>

Luttinger's theorem is obeyed: the area of the Fermi surface is the same as in the absence of interactions.<sup>104</sup> This means that even though there are strong electron-electron interactions, Hückel band structure calculations (which ignore the interactions) may still be able to predict the Fermi surface area correctly. It has often been found for the organics that Hückel calculations can produce Fermi surface areas in agreement with the frequency of magneto-oscillations.<sup>9</sup> This success should *not* be used to argue that the electron-electron interactions are weak.

In conclusion, many of the above properties are similar to those of the metallic phase of the  $\kappa$ -(BEDT-TTF)<sub>2</sub>X salts, particularly the presence of a low-energy scale below which Fermi liquid behavior is observed. The dynamical mean-field theory results for temperature and frequency dependences for the conductivity appear to be very similar to experimental results. Two notable differences exist between the dynamical mean-field theory results and properties of the  $\kappa$ -(BEDT-TTF)<sub>2</sub>X salts. First, the calculated value of the ratio  $A/\gamma^2$  is 5 to 200 times smaller than observed. Second, the nmr relaxation rate at low temperatures is not linear in temperature, as predicted by (17). It remains to be seen if these discrepancies occur because for these quantities the two-dimensionality of the organics becomes important.

### III. FUTURE DIRECTIONS

In conclusion, the experimental properties of this class of organic superconductors have been reviewed with an emphasis on similarities to the cuprates and how the metallic phase has properties quite distinct from a conventional metal. Quantum chemistry calculations can be used to justify a minimal microscopic model: a Hubbard model on an anisotropic triangular lattice. Appropriate parameters for this model suggest that there is substantial magnetic frustration and the system is close to a metal-insulator transition. Consequently, recent results for the Mott-Hubbard transition suggest that this model can explain the unconventional metallic properties. However, there are many details to be worked out and so below some specific suggestions are made for future theoretical and experimental work.

#### *Theory.*

Based on the above discussion Figure 6 shows a speculative phase diagram for the Hubbard model (7) at half-filling and zero temperature. The challenge is to determine the actual phase diagram using the arsenal of theoretical techniques that have been developed over the past decade to attack Hubbard models for the cuprates. Numerical techniques that could be used include exact diagonalization<sup>105</sup> and quantum Monte Carlo.<sup>105,106</sup> Analytic techniques that could be used include the fluctuation-exchange approximation<sup>107</sup> and slave bosons.<sup>108</sup> Insights might be gained from using ideas from gauge theory of fluctuations<sup>110</sup> and the SO(5) unified theory of superconductivity and antiferromagnetism.<sup>109</sup> The most important question is whether this Hubbard model can produce superconductivity. This is controversial for the square lattice model away from half-filling.<sup>106</sup> Other questions of interest include: Does the metallic phase have non-Fermi liquid properties? Are spin liquid phases possible?

It was shown in Section II F that dynamical mean-field theory can provide important insights into the organics. However, the connection with the model Hamiltonian (7) needs to be made more precise by working out the appropriate lattice of large connectivity or dimensionality to study. Possibilities include the infinite connectivity limit of the Bethe lattice with nearest neighbour and next-nearest neighbour hopping and the two-sublattice frustrated model.<sup>93</sup> In both these models the degree of magnetic frustration can be varied. Then the complete temperature dependence of resistivity, Hall resistance, thermopower, magnetic susceptibility, and nmr relaxation rate should be calculated and compared to the organics.

Finally, as discussed in Section 11 a better understanding is needed of how the model parameters vary with pressure.

#### *Experiment.*

The organics have a number of advantages over the cuprates for experimental study. First, since pressure and not doping is used to tune through the metal-insulator transition (compare Figure 8) only a single sample is needed to study the transition. Second, the lower superconducting transition temperature and high purity samples mean that magneto-oscillations provide a powerful probe of the Fermi surface. On the other hand, the single crystals are sufficiently small that neutron scattering is difficult and the first studies on the organics have only recently been performed.<sup>111</sup> Further studies could probe the magnetic fluctuations. X=Cu[N(CN)<sub>2</sub>]Br lies close to the metal-insulator transition<sup>29</sup> and so is the ideal candidate for further study. More systematic experimental studies of the metallic state and its variation with pressure are needed. Extensive transport and thermodynamic measurements should be made on the *same* single crystal. Of particular interest is how much of the low-temperature data can be explained within a Brinkman-Rice picture<sup>96</sup> of a Fermi liquid with an effective mass that diverges at the metal-insulator transition.

By applying uniaxial stress along the **c**-axis (in the conducting plane) it should be possible to vary the ratio of  $t_1$  to  $t_2$  and thus vary the magnetic frustration. A few uniaxial stress experiments<sup>112–114</sup> have been performed. One did find that for stress in the plane the resistivity peak and superconducting transition temperature were enhanced.<sup>113</sup> More extensive measurements are needed.

$X=\text{Cu}_2(\text{CN})_3$  is particularly interesting because in the insulating phase at ambient pressure there is no evidence of antiferromagnet ordering at low temperatures.<sup>13</sup> This should be checked with nuclear magnetic resonance. The magnetic susceptibility decreases rapidly below 10 K. Is this due to a spin liquid ground state? The parameter values in Table I suggest that this material has the largest amount of magnetic frustration of the listed materials.

## ACKNOWLEDGMENTS

This work was supported by the Australian Research Council and the USA National High Magnetic Field Laboratory which is supported by NSF Cooperative Agreement No. DMR-9016241 and the state of Florida. Helpful discussions with J. S. Brooks, R. J. Bursill, J. E. Gubernatis, J. Oitmaa, M. J. Rozenberg, J. R. Schrieffer, R. R. P. Singh, D. Vollhardt, and W. Zheng are gratefully acknowledged. I thank J. Eldridge and Y. Xie for providing the data shown in Figure 2. Perez Moses produced the figures.

*Note added in proof.* Since submission of this article preprints have appeared which consider the possibility of superconductivity in the Hubbard model on the anisotropic triangular lattice. Calculations at the level of the random-phase approximation (RPA) [M. Votja and E. Dagotto, cond-mat/9807168] and the fluctuation-exchange approximation [J. Schmalian, cond-mat/9807042; H. Kino and H. Kontani, cond-mat/9807147; H. Kondo and T. Moriya, cond-mat/9807322] suggest that at the boundary of the antiferromagnetic phase the model exhibits superconductivity mediated by spin fluctuations. This result is consistent with the speculative phase diagram shown in Figure 6 of this article. As the ratio  $t_1/t_2$  increases the wavevector associated with the antiferromagnetic spin fluctuations changes from  $(\pi, \pi)$  and the RPA calculations suggest that the superconductivity changes from d-wave singlet to s-wave triplet in the odd-frequency channel.

---

\* e-mail: ross@newt.phys.unsw.edu.au

- <sup>1</sup> For a review, P. Fulde, *Electron correlations in molecules and solids*, Third enlarged edition (Springer-Verlag, Berlin, 1995).
- <sup>2</sup> P. W. Anderson, *The Theory of Superconductivity in the High  $T_c$  Cuprates* (Princeton U.P., Princeton, 1997).
- <sup>3</sup> P. B. Allen, Comments Cond. Mat. Phys. **15**, 327 (1992).
- <sup>4</sup> R. H. McKenzie, Science **278**, 820 (1997).
- <sup>5</sup> For an earlier comparison of the organic and cuprate superconductors see, R. L. Greene, in *Organic Superconductivity*, edited by V. Z. Kresin and W. A. Little (Plenum Press, New York, 1990).
- <sup>6</sup> This point was also emphasized by Kanoda (Ref. 15).
- <sup>7</sup> H. Kino and H. Fukuyama, J. Phys. Soc. Jpn. **65**, 2158 (1996).
- <sup>8</sup> T. Ishiguro and K. Yamaji, *Organic Superconductors*, Second edition (Springer-Verlag, Berlin, 1997).
- <sup>9</sup> J. Wosnitza, *Fermi Surfaces of Low Dimensional Organic Metals and Superconductors* (Springer Verlag, Berlin, 1996).
- <sup>10</sup> J. M. Williams *et al.*, *Organic superconductors (including fullerenes) : synthesis, structure, properties, and theory* (Prentice Hall, Englewood Cliffs, 1992).
- <sup>11</sup> J. M. Williams *et al.*, Science **252**, 1501 (1991); D. Jerome, *ibid.* **252**, 1509 (1991).
- <sup>12</sup> H. Ito *et al.*, J. Phys. Soc. Japan **65**, 2987 (1996).
- <sup>13</sup> T. Komatsu *et al.*, J. Phys. Soc. Japan **65**, 1340 (1996).
- <sup>14</sup> K. Miyagawa *et al.*, Phys. Rev. Lett. **75**, 1174 (1995).
- <sup>15</sup> K. Kanoda, Physica C **282**, 299 (1997).
- <sup>16</sup> U. Welp *et al.*, Phys. Rev. Lett. **69**, 840 (1992).
- <sup>17</sup> Insight into this may be gained by considering the situation in the cuprates. When  $\text{La}_2\text{CuO}_4$  is doped it becomes a high- $T_c$  superconductor. The undoped material has an antiferromagnetic ground state with a small ferromagnetic moment. The latter arises because the  $\text{CuO}_6$  octahedra are slightly tilted giving rise to a spin-orbit interaction and Dzyaloshinskii-Moriya interaction. [L. O. Manuel *et al.*, Phys. Rev. B **54**, 12946 (1997) and references therein].
- <sup>18</sup> H. Ohta *et al.*, Synth. Metals **86**, 2079 (1997).
- <sup>19</sup> Yu. V. Sushko *et al.*, J. Superconductivity **7**, 937 (1994).

- <sup>20</sup> Yu. V. Sushko *et al.*, Synth. Metals **85**, 1541 (1997).
- <sup>21</sup> K. Kornelsen *et al.*, Solid State Commun. **72**, 475 (1989).
- <sup>22</sup> J. E. Eldridge *et al.*, *ibid.* **79**, 583 (1991).
- <sup>23</sup> M. Dressel *et al.*, Phys. Rev B **50**, 13603 (1994).
- <sup>24</sup> M. Tamura *et al.*, J. Phys. Soc. Jpn. **60**, 3861 (1991).
- <sup>25</sup> C. P. Slichter, *Principles of Magnetic Resonance*, Second edition (Springer Verlag, Berlin, 1978).
- <sup>26</sup> S. M. De Soto *et al.*, Phys. Rev B **52**, 10364 (1995);
- <sup>27</sup> H. Mayaffre *et al.*, Europhys. Lett. **28**, 205 (1994); Phys. Rev. Lett. **75**, 4122 (1995).
- <sup>28</sup> A. Kawamoto *et al.*, Phys. Rev B **52**, 15522 (1995).
- <sup>29</sup> A. Kawamoto, K. Miyagawa, and K. Kanoda, Phys. Rev B **55**, 14140 (1997).
- <sup>30</sup> M. Takigawa *et al.*, Phys. Rev. B **43**, 247 (1991).
- <sup>31</sup> M. Dressel *et al.*, Synth. Metals **85**, 1503 (1997).
- <sup>32</sup> K. Kadowaki and S. B. Woods, Solid State Commun. **58**, 507 (1986).
- <sup>33</sup> K. Miyake, T. Matsuura, and C. M. Varma, Solid State Commun. **71**, 1149 (1989).
- <sup>34</sup> Y. Tokura *et al.*, Phys. Rev. Lett. **70**, 2126 (1993).
- <sup>35</sup> T. T. M. Palstra *et al.*, Phys. Rev. B **50**, 3462 (1994).
- <sup>36</sup> M. Weger *et al.*, J. Phys.: Condens. Matter **5**, 8569 (1993).
- <sup>37</sup> M. Gurvitch, Phys. Rev. Lett. **56**, 647 (1986).
- <sup>38</sup> N. G. Ptitsina *et al.*, Phys. Rev. B **56**, 10089 (1997).
- <sup>39</sup> For a discussion of these issues for other organics see M. Weger, Phil. Mag. B **56**, 889 (1987).
- <sup>40</sup> N. F. Mott, *Metal insulator transitions*, (Taylor and Francis, London, 1990).
- <sup>41</sup> V. J. Emery and S. A. Kivelson, Phys. Rev. Lett. **74**, 3253 (1995); P. B. Allen *et al.*, Phys. Rev. B **53**, 4393 (1996); L. Klein *et al.*, Phys. Rev. Lett. **77**, 2774 (1996).
- <sup>42</sup> C. M. Hurd, *Hall Effect in Metals and Alloys* (Plenum, New York, 1972).
- <sup>43</sup> B. Andraka *et al.*, Solid State Commun. **79**, 57 (1991).
- <sup>44</sup> K. Murata *et al.*, Solid State Commun. **76**, 377 (1990).
- <sup>45</sup> M. A. Tanatar *et al.*, Phys. Rev B **55**, 12529 (1997).
- <sup>46</sup> T. R. Chien, Z. Z. Wang, and N. P. Ong, Phys. Rev. Lett. **67**, 2088 (1991).
- <sup>47</sup> P. W. Anderson, Phys. Rev. Lett. **67**, 2092 (1991).
- <sup>48</sup> P. Coleman, A. J. Schofield, and A. M. Tsvelik, Phys. Rev. Lett. **76**, 1324 (1996); J. Phys.: Cond. Matter **8**, 9985 (1996).
- <sup>49</sup> R. C. Yu *et al.*, Phys. Rev. B **44**, 6932 (1991).
- <sup>50</sup> J.-S. Zhou and J. B. Goodenough, Phys. Rev. B **51**, 3104 (1995).
- <sup>51</sup> B. Andraka *et al.*, Phys. Rev. B **40**, 11345 (1989).
- <sup>52</sup> R. C. Haddon, A. P. Ramirez, and S. H. Glarum, Adv. Mater. **6**, 316 (1994).
- <sup>53</sup> P. A. Lee *et al.*, Comments Cond. Mat. Phys. **3**, 99 (1986).
- <sup>54</sup> C. H. Mielke *et al.*, Phys. Rev. B **56**, R4309 (1997).
- <sup>55</sup> N. Harrison *et al.*, J. Phys.: Condens. Matter **8**, 5415 (1996).
- <sup>56</sup> J. Caulfield *et al.*, J. Phys.: Condens. Matter **6**, 2911 (1994).
- <sup>57</sup> J. Wosnitza *et al.*, Phys. Rev. B **45**, 3018 (1992).
- <sup>58</sup> K. Oshima *et al.*, Phys. Rev. B **38**, 938 (1988).
- <sup>59</sup> D. Schweitzer *et al.*, Synth. Metals **70**, 857 (1995); E. Balthes *et al.*, *ibid.* **85**, 1549 (1997).
- <sup>60</sup> W. Kohn, Phys. Rev. **123**, 1242 (1961).
- <sup>61</sup> S. Hill *et al.*, Synth. Metals **55-57**, 2566 (1993).
- <sup>62</sup> Y.-N. Xu *et al.*, Phys. Rev. B **52**, 12946 (1995); **55**, 2780 (1997).
- <sup>63</sup> D. J. Scalapino, Phys. Rep. **250**, 329 (1995).
- <sup>64</sup> K. Kanoda *et al.*, Phys. Rev. B **54**, 76 (1996).
- <sup>65</sup> Y. Nakazawa and K. Kanoda, Phys. Rev. B **55**, R8670 (1997).
- <sup>66</sup> G. E. Volovik, JETP Lett. **58**, 469 (1993); S. H. Simon and P. A. Lee, Phys. Rev. Lett. **78**, 1548 (1997); C. Kubert and P. J. Hirschfeld, Solid State Commun. **105**, 459 (1998).
- <sup>67</sup> M. Lang *et al.*, Phys. Rev. Lett. **69**, 1443 (1992).
- <sup>68</sup> L. P. Le *et al.*, Phys. Rev. Lett. **68**, 1923 (1992).
- <sup>69</sup> D. R. Harshman *et al.*, Phys. Rev. B **49**, 12990 (1994).
- <sup>70</sup> K. W. Kwok *et al.*, Phys. Rev. B **42**, 8686 (1990).
- <sup>71</sup> K. Oshima *et al.*, J. Phys. Soc. Japan **57**, 730 (1988).
- <sup>72</sup> U. G. L. Lahaise *et al.*, Phys. Rev. B **51**, 3301 (1995).
- <sup>73</sup> G. Visentini *et al.*, cond-mat/9706010.
- <sup>74</sup> U. Geiser *et al.*, Physica C **174**, 475 (1991).
- <sup>75</sup> A. Fortunelli and A. Painelli, J. Chem. Phys. **106**, 8051 (1997).
- <sup>76</sup> Y. Okuno and H. Fukutome, Solid State Commun. **101**, 355 (1997).
- <sup>77</sup> F. Castet, A. Fritsch, and L. Ducasse, J. Phys. I France **6**, 583 (1996).

- <sup>78</sup> H. Tajima *et al.*, Bull. Chem. Soc. Jpn. **63**, 538 (1990).
- <sup>79</sup> I. D. Parker *et al.*, J. Phys.: Condens. Matter **1**, 5681 (1989).
- <sup>80</sup> N. W. Ashcroft and N. D. Mermin, *Solid State Physics* (Saunders, Philadelphia, 1976), p. 689.
- <sup>81</sup> This effect was overlooked by Kino and Fukayama.
- <sup>82</sup> C. Jayaprakash *et al.*, Europhys. Lett. **15**, 625 (1991); M. Kato and F. Kokubo, Phys. Rev. B **49**, 8864 (1994).
- <sup>83</sup> C. J. Gazza, A. E. Trumper, and H. A. Ceccatto, J. Phys.: Condens. Matter **6**, L625 (1994).
- <sup>84</sup> U. Pecher and H. Büttner, Z. Phys. B **98**, 239 (1995), and references therein.
- <sup>85</sup> The physics and phase diagram of this model should be similar to that of the two-dimensional Hubbard model on a square lattice with hopping between nearest neighbours and along the plaquette diagonals (the  $t - t' - U$  model) at half-filling. A recent quantum Monte Carlo study presented evidence for an antiferromagnetic metallic phase between the paramagnetic metal and insulating antiferromagnetic phases [D. Duffy and A. Moreo, Phys. Rev. B **55**, R676 (1997)]. See also, W. Hofstetter and D. Vollhardt, cond-mat/9802233.
- <sup>86</sup> A. Auerbach, *Interacting Electrons and Quantum Magnetism*, (Springer - Verlag, New York, 1994).
- <sup>87</sup> R. R. P. Singh, O. A. Starykh, and P. J. Freitas, cond-mat/9710109.
- <sup>88</sup> P. W. Anderson, Mater. Res. Bull. **8**, 153 (1973).
- <sup>89</sup> N. Elstner, R. R. P. Singh, and A. P. Young, Phys. Rev. Lett. **71**, 1629 (1993); B. Bernu *et al.*, Phys. Rev. B **50**, 10048 (1994).
- <sup>90</sup> R. J. Bursill *et al.*, J. Phys.: Condens. Matter **7**, 8605 (1995); S. R. White and I. Affleck, Phys. Rev. B **54**, 9862 (1996), and references therein.
- <sup>91</sup> M. Rahal *et al.*, Acta Cryst. B **53**, 159 (1997).
- <sup>92</sup> C. E. Campos *et al.*, Phys. Rev. B **53**, 12725 (1996).
- <sup>93</sup> A. Georges, G. Kotliar, W. Krauth and M. J. Rozenberg, Rev. Mod. Phys. **68**, 13 (1996).
- <sup>94</sup> G. Moeller *et al.*, Phys. Rev. Lett. **74**, 2082 (1995).
- <sup>95</sup> M. J. Rozenberg *et al.*, Phys. Rev. Lett. **75**, 105 (1995).
- <sup>96</sup> W. F. Brinkman and T. M. Rice, Phys. Rev. B **2**, 4302 (1970).
- <sup>97</sup> Th. Pruschke, D. L. Cox, and M. Jarrell, Phys. Rev. B **47**, 3553 (1993).
- <sup>98</sup> M. J. Rozenberg *et al.*, Phys. Rev. Lett. **76**, 4781 (1996).
- <sup>99</sup> M. J. Rozenberg, G. Kotliar and H. Kajueter, Phys. Rev. B **54**, 8452 (1996).
- <sup>100</sup> P. Majumdar and H. R. Krishnamurthy, Phys. Rev. B **52**, R5479 (1995).
- <sup>101</sup> Th. Pruschke, M. Jarrell, and J. K. Freericks, Adv. Phys. **44**, 187 (1995).
- <sup>102</sup> P. Majumdar and H. R. Krishnamurthy, cond-mat/9512151.
- <sup>103</sup> C. H. Pennington and C. P. Slichter, Phys. Rev. Lett. **66**, 381 (1991); A. Sokol, R. L. Glenister, and R. R. P. Singh, *ibid.* **72**, 1549 (1994).
- <sup>104</sup> E. Müller-Hartmann, Z. Phys. B **76**, 211 (1989).
- <sup>105</sup> E. Dagotto, Rev. Mod. Phys. **66**, 763 (1994).
- <sup>106</sup> S. Zhang, J. Carlson, and J. E. Gubernatis, Phys. Rev. Lett. **78**, 4486 (1997); W. Fettes and I. Morgenstern, cond-mat/9801227.
- <sup>107</sup> N. E. Bickers and D. J. Scalapino, Ann. Phys. (N.Y.) **193**, 206 (1989); M. Langer *et al.*, Phys. Rev. Lett. **75**, 4508 (1995); J. J. Deisz, D. W. Hess, and J. W. Serene, Phys. Rev. Lett. **76**, 1312 (1996).
- <sup>108</sup> X.-G. Wen and P. A. Lee, Phys. Rev. Lett. **76**, 50 (1996) and references therein.
- <sup>109</sup> S.-C. Zhang, Science **275**, 1089 (1997).
- <sup>110</sup> D. H. Kim, D. K. K. Lee, and P. A. Lee, Phys. Rev. B **55**, 591 (1997).
- <sup>111</sup> L. Pintschovius *et al.*, Europhys. Lett. **37**, 627 (1997); N. Toyota *et al.*, Synth. Metals, **86**, 2009 (1997).
- <sup>112</sup> C. E. Campos *et al.*, Physica B **211**, 293 (1995).
- <sup>113</sup> H. Kusunohara *et al.*, Solid State Commun. **74**, 251 (1990).
- <sup>114</sup> M. Kund *et al.*, Synth. Metals **70**, 949 (1995).
- <sup>115</sup> P. Wzietek *et al.*, Synth. Metals **85**, 1511 (1997).

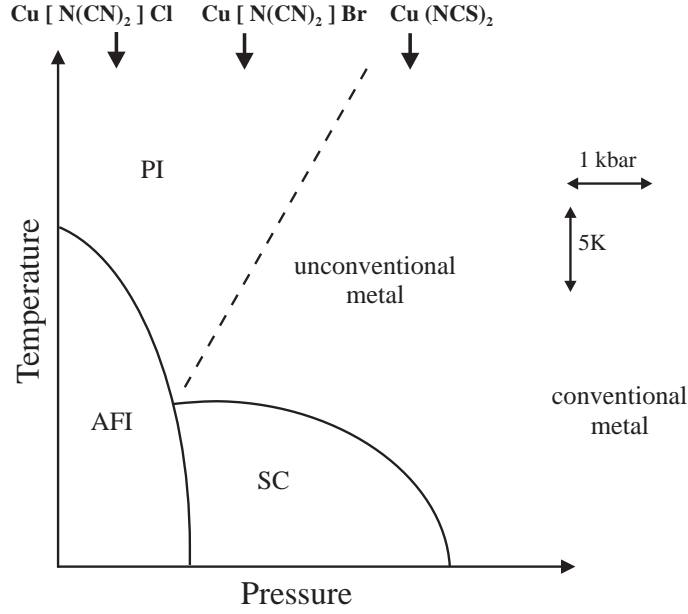


FIG. 1. Schematic phase diagram of the  $\kappa$ -(BEDT-TTF) $_2$ X family of organic conductors.<sup>7,15,115</sup> AFI denotes an insulating antiferromagnetic phase, PMI an paramagnetic insulating phase, and SC a superconducting phase. The phase transition between the paramagnetic phases is first order and denoted by the dashed line which ends at a second order critical point. The arrows denote the location of at ambient pressure of materials with different anions X. As the pressure increases the unconventional properties of the metallic phase disappear. The above phase diagram is qualitatively similar to that of the cuprate superconductors with doping playing the role of pressure.

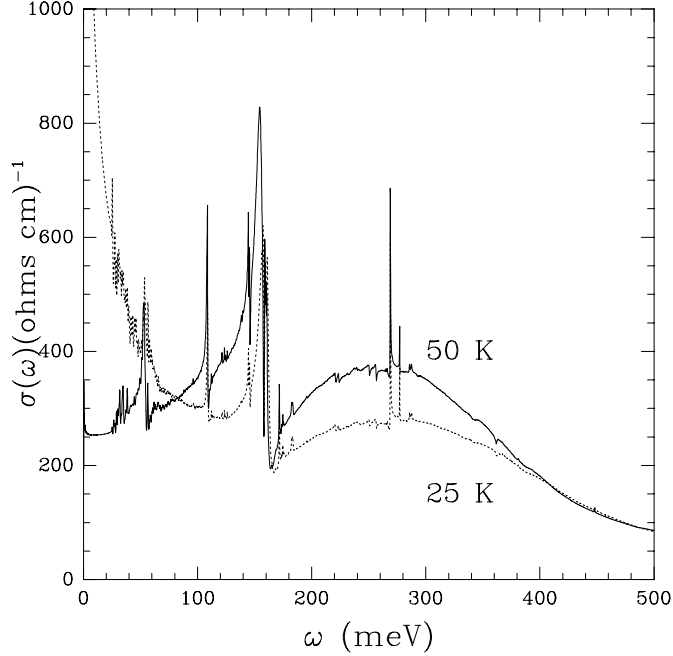


FIG. 2. Non-Drude behavior of the frequency-dependent conductivity  $\sigma(\omega)$  of  $X=\text{Cu}[\text{N}(\text{CN})_2]\text{Br}$ . The data is from Reference 21 and shows the strong temperature dependence of the low-frequency conductivity. At 25 K and below  $\sigma(\omega)$  has a Drude-type peak at zero frequency (see the dashed curve). In contrast, this peak is completely absent at 50 K and above (see the solid curve). The broad peak around 300 meV can be identified with transitions between the lower and upper Hubbard bands. The very sharp features are due to infra-red active phonons. The data shown is for the electric field parallel to the **a**-axis. Similar data is obtained for the electric field parallel to the **c**-axis except the broad peak is around 400 meV.<sup>21</sup> (Both the **a**-axis and the **c**-axis are in the plane of the layers).

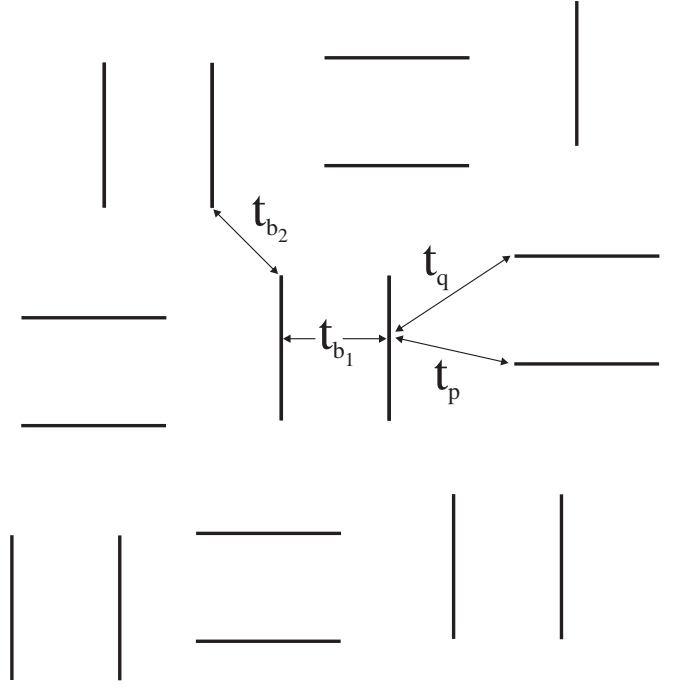


FIG. 3. Geometrical arrangement of the BEDT-TTF molecules in the conducting layers of the  $\kappa$  phase. Each line represents a BEDT-TTF molecule. The dominant intermolecular hopping integrals are shown. Some calculated values for these integrals are given in Table 1.

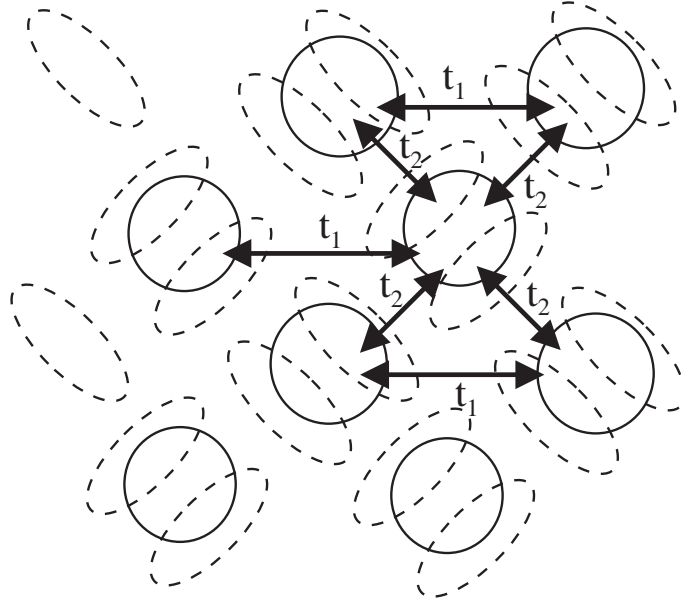


FIG. 4. Triangular lattice for the dimer model of  $\kappa$ -(BEDT-TTF)<sub>2</sub>X. Each lattice site is denoted by a circle and represents the anti-bonding orbital on a dimer, a pair of BEDT-TTF molecules. Each dashed oval represents a single BEDT-TTF molecule. There is no hopping in the vertical direction and there is hopping along the diagonals. Competition between the two types of hopping results in magnetic frustration and a Mott-Hubbard metal-insulator transition at a critical value of the Coulomb repulsion.

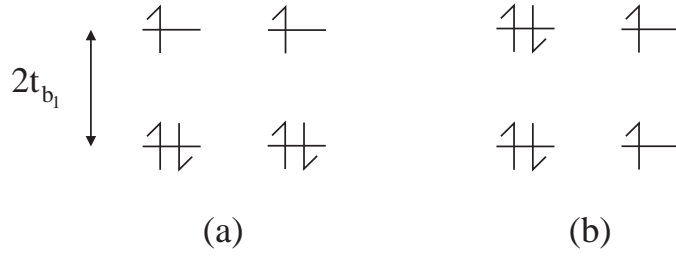


FIG. 5. Effective Coulomb repulsion between two electrons in the anti-bonding orbital of a dimer in the strongly correlated limit. (a) The ground state of a pair of three-quarter filled dimers. If  $t_{b_1}$  is the intradimer hopping integral then  $2t_{b_1}$  is the energy splitting of the bonding and anti-bonding orbital. (b) If the Coulomb repulsion  $U_0$  on a single molecule is much larger than  $t_{b_1}$  then this denotes the configuration of the lowest energy configuration involving charge transfer between dimers. The energy difference between (a) and (b) is  $2t_{b_1}$  and so this is the effective Coulomb repulsion on a dimer for  $U_0 \gg t_{b_1}$ .

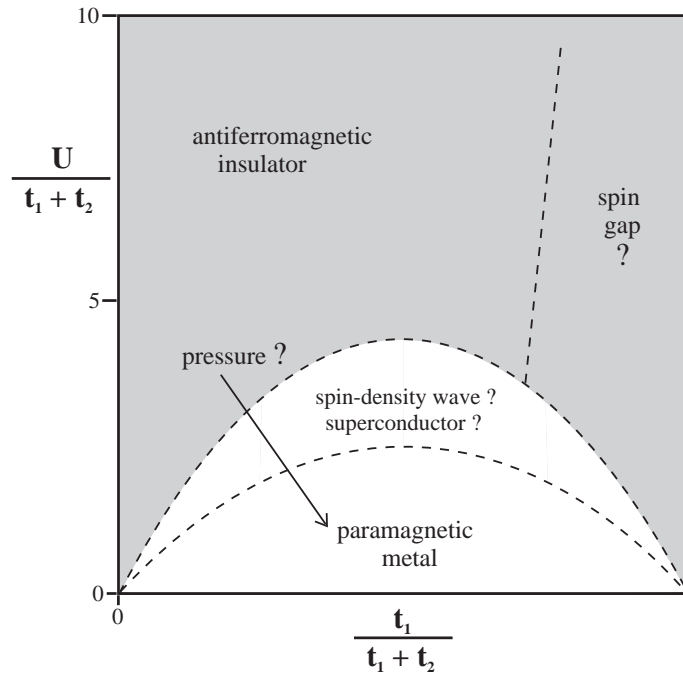


FIG. 6. Speculative phase diagram for the Hubbard model on an anisotropic triangular lattice (7). Shaded and unshaded areas represent insulating and metallic regions respectively. The solid line with an arrow shows how the ground state of a particular  $\kappa$ -(BEDT-TTF)<sub>2</sub>X crystal might change as the pressure is increased. Vertical lines on the left side, center, and right side correspond to the Hubbard model on a square lattice, triangular lattice and decoupled chains, respectively.

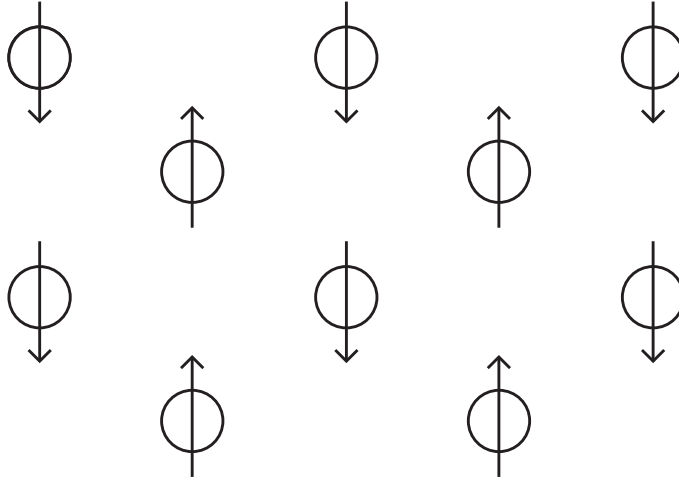


FIG. 7. Collinear spin structure of the antiferromagnetic ground state for the dimer model (7) with  $t_1 \ll t_2 \ll U$ . Each circle represents a dimer of BEDT-TTF molecules. This is the same structure as that proposed for deuterated  $\text{X}=\text{Cu}[\text{N}(\text{CN})_2]\text{Br}$  based on nmr measurements.<sup>15</sup>

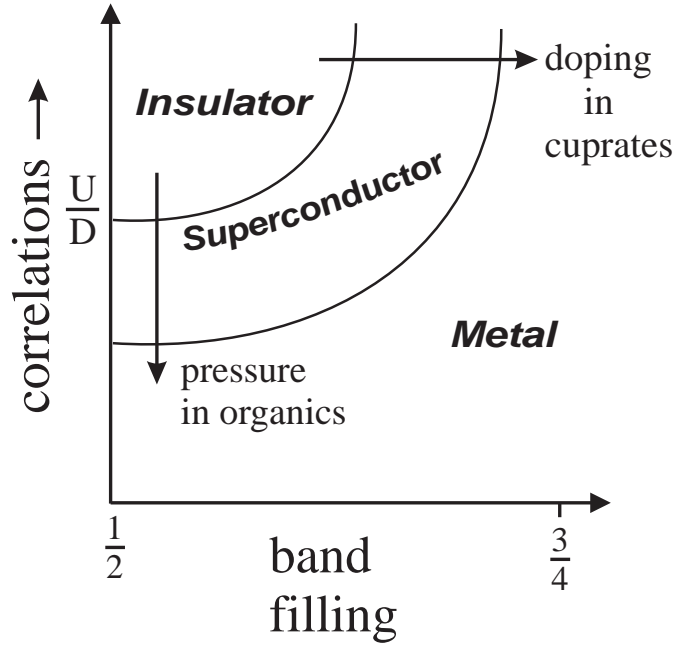


FIG. 8. A simple unified picture of the phase diagram of the organics and cuprates at low-temperatures. The organic superconductors  $\kappa\text{-(BEDT-TTF)}_2\text{X}$  are always at half-filling and one tunes through the insulator-superconductor-metal transition by applying pressure. In the cuprates this transition is passed through by varying the band filling.

TABLE I. Values of the hopping integrals (in meV) between the BEDT-TTF molecules in the  $\kappa$ -(BEDT-TTF)<sub>2</sub>X crystal structure for different anions X. All values were based on quantum chemistry calculations using the Hückel approximation, except the first line which involved an *ab initio* calculation. All values are for the crystal structure at ambient pressure, unless denoted otherwise. The parameters in the Hubbard model (7) are given by  $t_1 \sim t_{b_2}/2$ ,  $t_2 \sim (t_p + t_q)/2$ , and  $U \sim 2t_{b_1}$  (See equations (6) and (8)). The fact that  $t_1 \sim t_2$  implies that there is significant magnetic frustration. Note that for the same anion there is some variation between the values of the hopping integrals calculated by different researchers.

Anion X	$t_{b_1}$	$t_{b_2}$	$t_p$	$t_q$	$t_1/t_2$	Ref.
Cu[N(CN) <sub>2</sub> ]Br	272	85	130	40	0.50	75
Cu[N(CN) <sub>2</sub> ]Br	224	71	94	40	0.53	75
Cu[N(CN) <sub>2</sub> ]Br	244	92	101	34	0.68	13
Cu(CN) <sub>3</sub>	224	115	80	29	1.10	13
I <sub>3</sub>	247	88	119	33	0.58	13
Cu(SCN) <sub>2</sub>	230	113	99	33	0.85	13
Cu(SCN) <sub>2</sub>	136	50	41	27	0.74	91
Cu(SCN) <sub>2</sub> (7.5 kbar)	162	54	58	30	0.61	91
Cu(SCN) <sub>2</sub>	244	26	22	20	0.62	92
Cu(SCN) <sub>2</sub> (20 kbar)	324	45	27	31	0.88	92